

## Study of Structural / Optical Properties of Aluminum Doped CoO [ACO] Thin Films.

K.U.POkpechi\*, A.D Asiegbu, C.I Oriaku, C.E.Nwokorongwo,  
Ugochukwu Joseph

Department of Physics Michael Okpara University of Agriculture, Umudike  
P.M.B 7267, Umuahia, Abia State, Nigeria

---

### Abstract:

Al Doped CoO thin film [ACO] were successfully deposited on amorphous glass substrate using Successive Ionic Layer Adsorption and Reaction deposition method [SILAR]. The deposited film were annealed at temperature of 300°C and the annealed time varied for 1hr, 1hr.15mins, 1hr.30mins, 1hr.45mins and 2hrs. Thin films of ACO were deposited on glass by successive immersion of the substrate into a complex (NH<sub>4</sub>) AlCoCl<sub>2</sub> bath kept at room temperature. 3ml of 3M solution of ammonia (NH<sub>4</sub>) used as a complexing agent was measured and added into a beaker with 40.0g of 0.6M of CoCl to form a complex cobalt ion, 10% of AlCl<sub>2</sub> was also measured and added as a dopant, 30ml NaOH containing 37.2g of 0.5M of NaOH was also prepared and pour into a separate beaker. 30mls of ion exchange water was also poured into two separate beakers. The pH of the solution was measured to be 8.0. The optical properties were characterized using UV-1800 double beam spectrophotometer and the crystallographic studies were done using X-ray diffractometer and Scanning electron microscope. In our study, the thin films show very low absorption with high optical transmittance in the visible, ultraviolet region of the spectrum between 700 -900nm. The crystallographic structure shows an interconversion between CoO and Co<sub>3</sub>O<sub>4</sub> peaks at the surface which are cubic and cubic spinel crystalline in nature. The Scanning Electron Micrograph shows that the grain size were evenly distributed with porous structure.

### Background:

Cobalt oxide thin films have attracted many research effort in recent years due to their potential application in various technological areas. They can be used as high temperature solar selective absorbers [11], anodic electrochromic materials in smart window devices [13] and negative electrodes in lithium-ion batteries [14]. Cobalt oxide exists in three different crystalline forms, namely CoO, Co<sub>2</sub>O<sub>3</sub> and Co<sub>3</sub>O<sub>4</sub>. [15]; Co<sub>3</sub>O<sub>4</sub> spinel structure contains vacancy and it is chemically stable. CoO phase has a high chemical stability but easily oxidized to Co<sub>3</sub>O<sub>4</sub> in the open air atmosphere. Cobalt oxides are one of the most important transition oxides which have huge interest in several fields. It is a p-type cubic spinel structure semiconducting material with two direct and indirect optical band gaps (1.44-2.06) eV and (1.26-1.38) eV respectively. Many researches has widely studied Co<sub>3</sub>O<sub>4</sub> Phase in open air atmosphere as promising materials due to its chemical stability, an antiferromagnetic material with mixed valence (Co<sup>3+</sup> and Co<sup>2+</sup> ion) and regular spinel structure having Co<sup>3+</sup> in Octahedral sites and Co<sup>2+</sup> in Tetrahedral sites. Both Co<sub>3</sub>O<sub>4</sub> and CoO exhibit a cubic lattice and usually nonstoichiometric with excess oxygen, leading to p-type semiconducting behaviors [3]. Aluminum is a post transition metal [a metalloid] which produces up to +3 ions. its usefulness in modern society include power lines, window frames, high rise building, electronics aircraft components, spacecraft components and in house hold and industrial appliances. Its high strength and low weight and corrosion resistance has made it an important material in technology. [1] Therefore, in this work, we studied structural and optical properties of CoO thin films by doping with aluminum oxide, annealed at 300°C with variation in annealing time of 1hr, 1.15mins, 1.30mins, 1.45mins, and 2hrs using SILAR method.

**Key Word:** [Aluminum, Cobalt oxide, thin films, Annealing time,]

---

Date of Submission: 10-07-2021

Date of Acceptance: 26-07-2021

---

### I. Introduction

The rapid development of communities across the world and the increase in energy consumption show that we will require more energy in the future. In the context of energy crisis, solar energy is an attractive source. It is plentiful, virtually inexhaustible and can provide more than enough energy to our society. However, the problem with producing electricity and fuels from solar energy is that it is still expensive, primarily from the materials used in the cells production. Thin film technology has broad range of utilization in various areas. It is a base of outstanding developments in the various fields of engineering, science and technology such as solid-state electronics, optics, magnetism, coatings, supercapacitor and photovoltaic (PV) cells. The importance of

thin film devices over the bulk materials are low material consumption, easy processing and possible use of flexible substrates (7). Magnetic oxide semiconductors are class of materials that are extremely low cost, abundant and can be created at the scale needed to meet widespread demand of the society. The synthesis and studies of nanosized materials have been intensively pursued in the recent years not only because of their characterization interest but also for their interesting properties such as catalytic, thermal, magnetic, electrical and optical properties and the variety of applications related to them. In the recent years, various techniques have been established for the establishment of nanostructured transition metal oxides thin films: physical and chemical vapor depositions, soft-chemistry methods etc. The transition metal thin films are important class of materials and the exhibit very interesting properties for uses in sensors, fuel cells, catalysis, solar cells, transformers, etc. Simultaneously to the search for solar cell efficiency improvements, (8) Cobalt Oxide based solar cells have the potential to counteract all the difficulties encountered in the usual solar cells. The all-oxide photovoltaic/ optoelectronic method is very captivating as a result of its chemical strength, negligible toxicity and large quantity of several metal oxides that possibly permits production of solar cells under ambient conditions. It can be utilized as constituents in photovoltaic cells like translucent conducting front electrodes or electron-transport layers [10]. Transition metal oxides are of technically and potentially important class of materials which have been widely researched as a result of their physio-chemical and material properties can be altered to cope up with the desired application potential. It is proposed here to synthesize by SILAR method, and study nanoparticles of new oxides of Cobalt, with controlled size and morphology, for processing as thin films that could be easily integrated in an energetic system of conversion. Various metal oxide schemes will drive to suitable physical characteristics such as the energy gap, sunlight absorption and different applications, firstly for optoelectronic and photovoltaic. Dopants are utilized in a metal oxide to modify or improve its properties. Therefore, the main objective of this work is to develop and study Al doped CoO material for possible application based on the structure and optical properties and their applications.

## II. Material And Methods

### EXPERIMENTAL DETAILS

3ml of 3M solution of ammonia used as a complexing agent was measured and added into a beaker with 30ml of (NH<sub>4</sub>)CoCl<sub>2</sub> containing 40.0g of 0.6M of CoCl and %10 of AlCl<sub>2</sub>, to form a complex cobalt ion, 30ml NaOH containing 37.2g of 0.5M of NaOH was also prepared and poured into a separate beaker. 30mls of ion exchange water was also poured into another beaker. The pH of the solution was measured to be 8.0. Thin films of AlCoO were deposited on glass by successive immersion of the substrate into a (NH<sub>4</sub>) AlCoCl<sub>2</sub> bath kept at room temperature and into a deionised water.

The cleaned glass substrate was immersed in the cobalt complex (at room temperature) for a known standardized time (20secs) followed by immersion into ion exchange water for 5secs for hydrogenation. It is then immersed into the NaOH solution for 20secs and back into ion exchange water. This cycle was repeated for 20 times in order to achieve a desired result. The decomposition of CoCl<sub>2</sub> in neutral aqueous solution (deionized water) will release ions of Al<sup>3+</sup>, Co<sup>2+</sup>, and OH<sup>-</sup> into solution and result in the formation of AlCo(OH)<sub>2</sub> or AlCoO particles. The [ACO] thin film were annealed at a temperature of 300°C at varied time of 1hr, 1.15mins, 1.30mins, 1.45mins, and 2hrs.

Below is the chemical reaction related to this process a dynamic equilibrium exists in the precursor under the influence of ammonia as the complexing agent. The chemical composition of the reaction:



During the reaction process in deionized water, complex [Co(NH<sub>3</sub>)<sub>4</sub>]<sup>2+</sup> decomposes with the final formation of [Co(OH)<sub>2</sub>] precipitation.



### ANALYSIS OF CRYSTALLINE STRUCTURE BY X-RAY DIFFRACTION (XRD)

The interaction of the incident rays with the sample produces constructive interference (and a diffracted ray) when conditions satisfy Bragg's Law [4].

$$= 2 \sin$$

Where,  $\theta$  is the angle between the primary X-ray beam (with wavelength),  $d$  is the interplaner spacing; and  $n$  is an integer. This law relates the wavelength of an electromagnetic radiation to the diffraction angle and the lattice spacing in a crystalline sample. The characteristic X-ray diffraction pattern generated in a typical XRD analysis provides a unique "signal" of the crystalline phase(s) present in the sample. When properly interpreted, by comparison with standard reference patterns and measurements, this signal allows identification of the crystalline form. The analyses by X-ray diffraction thin films were conducted to allow phase identification for the different synthesized oxides. The XRD was carried out using X-ray diffractometer modeled

GBC Enhanced Mini Material Analyzer (EMMA). It gives information relating to the nature and structure of the doped thin films of ACO. The crystallite size was obtained by the resolution of Scherrer's equation [9]:

$$D_{(h)} = K\lambda/B\cos\theta$$

Where:

$D_{(hkl)}$ : The average crystallite or particle size in a direction of plane (hkl) (nm)

$\lambda$ : The X-ray wavelength (nm) Where  $\lambda$  is the wavelength of Cu-K $\alpha$  radiation ( $\lambda=1.54060 \text{ \AA}$ )

K: A dimensionless shape factor ( $K = 0.94$ )

B: Full Width at Half Maximum (FWHM) of the diffraction peak (rad)

$\theta$ : Bragg diffraction angle (deg)

The lattice parameter which refers to the physical dimension of unit cells in a crystal lattice with three lattice constants for three dimensional lattices denoted by a, b, c for the thin films was calculated for different phases of the materials deposited.

Hexagonal phase formula (12):

$$\frac{1}{d^2} = \frac{4}{3} \left( \frac{h^2 + hk + k^2}{a_0^2} \right) + \frac{l^2}{c_0^2}$$

For cubic phase, the lattice constant was calculated from

Where d is the interplaner distance and hkl is the miller indices.

For tetragonal phase of the crystal structure

The micro strain was calculated using:

$$\epsilon =$$

The dislocation density (d) was determined using

$\delta$  = where d is the crystallite size

The volume for simple cubic was calculated from

$$V = a^3$$

For hexagonal structure

$$V = ()$$

For tetragonal structure

$$V = a^2c$$

## **MICROSTRUCTURAL ANALYSIS BY SCANNING ELECTRON MICROSCOPE (SEM)**

SEM is an apparatus that can take surface and cross-sectional images of the thin films by a scanning focused electron beam over a surface to create an image. The signals that are derive from electron-sample interactions reveal information about the sample including morphology (texture), chemical composition (using the Energy Dispersive Spectrophotometer analyzer), crystalline structure and orientation. In this work, Scanning electron microscope phenomprox, Model number MVEO16477830 manufactured by Phenom World Eindhoven Netherland Electron was used.

In the scanning electron microscope an electron beam, which is highly focused (spot size ~ 0.4 to 0.5 nm), is moving over each point of the object. This electron beam, with an energy ranging from 0.2 keV to 40 keV, is focused by one or two condenser lenses to a spot of about 0.4 nm to 5 nm in diameter. The beam passes through pairs of scanning coils or pairs of deflector plates in the electron column, typically in the final lens, which deflect the beam in the x and y axes so that it scans in a rectangular area of the sample surface. The surface and cross-sectional views of the thin films can be observed by SEM. Prior to observation, the sample was fixed to a sample holder with the surface to be analyzed facing up. The border of the sample was covered by a silver paste to facilitate the electron flow. On the observing surface, gold was deposited by cathodic sputtering to increase the conductivity of the surface. With this analysis, the surface and grain morphologies were observed.

## **OPTICAL ANALYSIS**

In this work, the optical performances of the thin films, which essentially consist of the absorbance, transmittance and reflectance, were studied using UV1-1800 series double beam spectrophotometer. The absorbance of the deposited films was measured using UV-spectrophotometer and occurred in the spectral range of 300nm-900nm of the electromagnetic spectrum. Other spectral/Optical parameters such as transmittance, reflectance, etc. were estimated using appropriate mathematical formulas given below:

a) Transmittance:

The values of absorbance were converted to transmittance using:

%T = antilog (2- absorbance)

b) Reflectance (R):

The reflectance was estimated using the equation [6].

$$1 = A + T + R$$

Where A is the absorbance, T is the transmittance and R is the reflectance of the deposited films.

For normalization, equation above becomes

$$1 = A + T + R$$

$$R = 1 - (T + R)$$

c) Absorption coefficient;

$$\alpha = \ln (1/T)$$

was used to deduce the absorption coefficient of the thin film.

d) Optical energy band gap ( $E_g$ )

The relationship between the absorption coefficient ( $\alpha$ ) and incident photon energy ( $h\nu$ ) can be determined using well known Tauc's relations [7]

$$(\alpha h\nu) = A (h\nu - E_g)^n$$

Where  $\nu$  is the frequency of the incident photon,  $h$  is the Planck's constant,  $A$  is a constant,  $E_g$  is the optical band gap and  $n$  is the transition type.

It has been established that for direct allowed band gap semiconductors, the measured absorption data fits well to for  $n = 1/2$ .

$$(\alpha h\nu) = A (h\nu - E_g)^{1/2}$$

Taking Square of both sides of the equation, we have

$$(\alpha h\nu)^2 = A(h\nu - E_g)$$

Hence, the graph of  $(\alpha h\nu)^2$  against  $h\nu$  was plotted and values of optical band gap energies  $E_g$  were obtained from extrapolating the straight portion of the graphs on the photon energy ( $h\nu$ ) axis at  $(\alpha h\nu)^2 = 0$  [3].

e) Extinction coefficient (k)

The extinction coefficient (k) of the films was determined using the equation for semi-conductors and insulators [10]

$$K = \alpha\lambda/4\pi$$

Where  $\alpha$  is the absorption coefficient of the thin film and  $\lambda$  is the wavelength of the incident electromagnetic radiation.

f) Refractive index (n)

The relationship between the index of refraction ( $n_s$ ) and the film reflectance (R) was used to estimate the refractive index [1];

$$R = (n_s - 1)^2 / (n_s + 1)^2$$

simplifying

$$n = (1 + (R)^{1/2}) / (1 - (R)^{1/2})$$

g) Dielectric constant ( $\epsilon$ )

The complex dielectric constant ( $\epsilon$ ) is given by [6];

$$\epsilon = \epsilon_r + \epsilon_i = (n + jk)^2$$

Where  $\epsilon_r$  = real part,  $\epsilon_i$  = imaginary part,  $n$  = refractive index and  $k$  = extinction coefficient.

Expanding, we obtain;

$$\epsilon = \epsilon_r + \epsilon_i = (n^2 - k^2) + 2njk$$

Equating the real and imaginary parts of the equation, we have that,

$$\epsilon_r = (n^2 - k^2) \text{ ----- The real part}$$

$$\epsilon_i = 2nk \text{ ----- The imaginary part}$$

h) Optical conductivity ( $\sigma_o$ )

The optical conductivity was estimated by the equation [8];

$$\sigma_o = \alpha nc / 4\pi$$

Where  $c$  is the speed of light in vacuum,  $\alpha$  is the absorption coefficient and  $n$  is the index of Refraction of the film.

### III. Results

#### Optical properties

The optical properties of the ACO thin films were examine using uv-spectrophotometer in the visible –ultraviolet near infrared region of the spectrum. Figure 3.1 explains the absorption property of the film.

At lower wavelength the films were found to be dark compound but became transparent at higher wavelength in the visible - infra red region. The film increased from 0.03 in the region of 700nm to 1.0 at 790nm. C3 shows zero absorbance from 700 to 740 but started increasing from 760nm. In Figure 3.2, the transmittance decreases sharply from 95% along the visible region of 720nm -760nm but drops sharply at 800nm. C3 has 100% transmittance at the wavelength of 700 to 740 in the visible region. In most cases optical parameters change with the thickness. it was also observed that the transmittance decreased with increased in thickness. This is in line with Beer- lambert law which reads

$$I_z = I_0 \exp(-\alpha Z)$$

Where I is the intensity, Z is the propagation direction,  $I_0$  is the initial amplitude of the intensity or absorption Coefficient. This means that the intensity decreases exponentially with propagation through the material and the absorbance of the film with thickness Z.

$$A(z) = 1 - \exp(-\alpha z)$$

Figure 3.3 explains the reflectance which has sharp peak at 21% in the wavelength of 790nm. And also small peak at the wavelength of 760nm. The reflectance shows a particular pattern throughout the films.

Figure 3.5 shows the absorption coefficient  $\alpha$  of the film in  $\text{cm}^{-1}$  with low values which decreases with annealing time. The low value in the absorption coefficient means that light is only poorly absorbed by the thin films of ACO and so, may not be good materials for application in thin film solar absorber. Figure 3.5a and 3.5b, explains the band gap of the thin films of ACO. The band gap of 1.6 eV was observed for all samples in time. Thus the band gap was not affected by the increase in annealing time. This may be as a result of constant doping concentration of 10%, and constant temperature of 300°C. Figure 3.4 explains the refractive index of the film, which is in range of 1.22 to 1.23. This could be as a result of the doping concentration and increase in the annealing time. Figure 3.6 and Figure 3.7 explains the dielectric constant of the thin films of ACO, which has a low dielectric constant and can be good materials for parasitic capacitance, enabling faster speeds and lower heat dissipation. They can be subjected to high electric field without breaking down. Figure 3.8 explains the extinction coefficient of the film and shows that light absorption is also poor throughout the wavelength of the film thus having a weak absorption. Since the material transmits in the visible band of 720nm and transmission is above 80% with a low index of refraction in the range of 1.2, it could have possible application in visible and thermal imaging and also in laser [3].

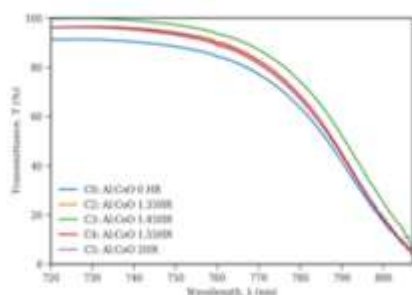


Fig 3.1: transmittance as a function of wavelength for ACO thin film annealed at different time

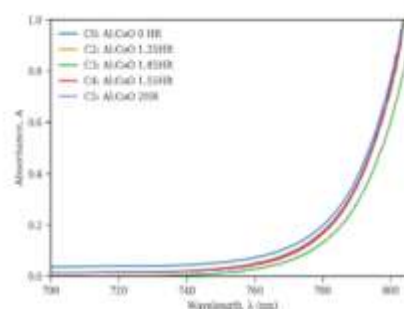


Fig3.2: Absorbance as a function of wavelength for ACO thin film annealed at different time

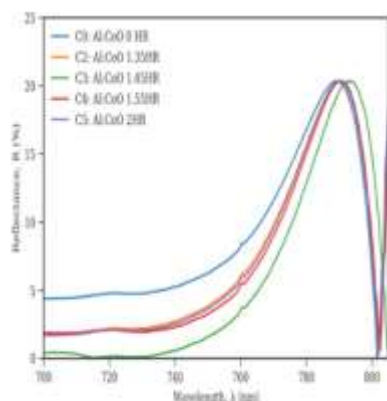


Fig 3.3: Absorbance as a function of wavelength for ACO thin films annealed at different time

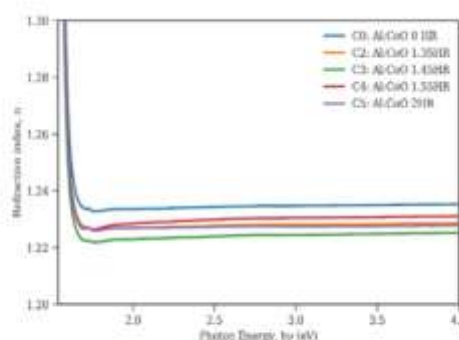


Figure 3.4: Plot of Refractive index versus photon energy of ACO for different annealing time

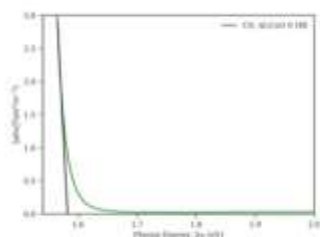


Figure 3.5a: Plot of  $(\alpha h\nu)^2$  versus photon energy for unannealed ACO

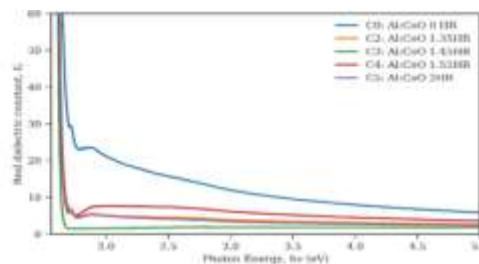


Figure 3.6: Plot of real dielectric constant versus photon energy of ACO for different annealing time

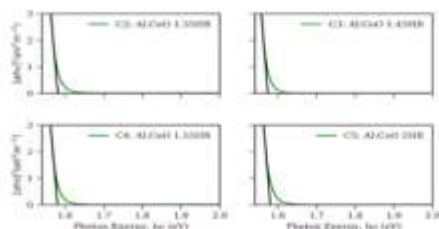


Figure 3.5b: Plot of  $(\alpha h\nu)^2$  versus photon energy of versus ACO for different annealing time.

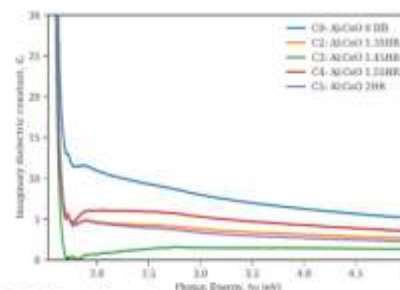


Figure 3.7: Plot of imaginary dielectric constant versus photon energy of ACO for different annealing time

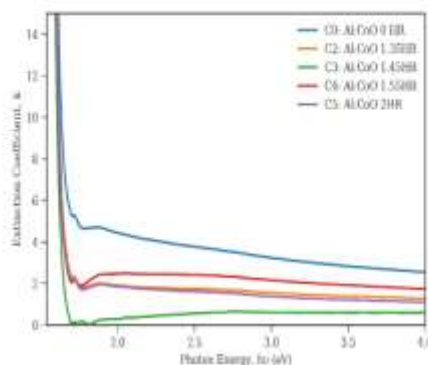


Figure 3.8: Plot of extinction coefficient versus photon energy of ACO for different annealing time.

Table 1: XRD parameters for ACO annealed for 1hr and 2hrs.

| LATTICE CONSTANT A° | DISLOCATION DENSITY | MICROSTRAIN $\epsilon$ | UNIT CELL VOLUME (cm <sup>3</sup> ) | av crystallite size(nm) |
|---------------------|---------------------|------------------------|-------------------------------------|-------------------------|
| C 1 ) 8 . 2 2 0 7 0 | 3 9 7               | 1 7 . 0 0 9 8          | 3 6 3 . 5 5 0                       | 1 1 7                   |
| C 5 ) 7 . 1 3 7 1 0 | 4 0 5 8             | 1 1 . 6 4 7 5          | 8 1 . 1 8 8 4 1                     | 8 8                     |

### Structural characterizations

The structural characterizations of ACO thin films have been examined by X-ray diffraction technique, to study the variations of the crystallinity. The XRD patterns of ACO thin films are shown in Figure 3.9 .This displayed the curved line of varied films with intensity. It was noticed that the samples were polycrystalline with the appearance of some XRD peaks reflections corresponding to a simple cubic phase CoO and simple cubic spinel structure Co<sub>3</sub>O<sub>4</sub> of the ACO thin film annealed at 300°C at 1hr and 2hrs. The diffraction peaks were growth along the inter planar spacing values for CoO corresponding to (220) and (311) diffraction planes, at  $2\theta = 62.539^\circ$  and  $72.129^\circ$  respectively. Co<sub>3</sub>O<sub>4</sub> With peaks at  $33.2^\circ, 49.5^\circ, 54.2^\circ, 64.1^\circ$ , their hkl correspondence are 220,222,422.and 440 .XRD patterns were ensured in comparison with ICDD card No. (78-0431) [5]. Traces of

aluminum were seen at peaks of  $2\theta = 24.2^\circ$ , and  $35.6^\circ$ , with hkl along (012) and (111) diffraction planes. At 2hrs, the phase of Crystallinity consist of  $\text{Co}_3\text{O}_4$  and  $\text{CoO}$ . With  $\text{CoO}$  peaks at  $2\theta = 41.^\circ$ , and  $62.0^\circ$ , their hkl correspondence are, 200, and 220, the XRD pattern shows the peaks of  $\text{Co}_3\text{O}_4$  at  $2\theta = 30.0^\circ, 36.4^\circ, 54.0^\circ, 64.0^\circ, 72.0^\circ$ . The aluminum traces were also seen with increased peaks at  $24.3^\circ$ ,  $34.0^\circ$  and  $48.5^\circ$  and their hkl at 012, 104, and 113. There is a good agreement in the observed and standard values of d-spacing of ACO thin films. There is an accuracy of about 95.5% in the matching process of XRD data with the database. Moreover,  $\text{CoO}$  and  $\text{Co}_3\text{O}_4$  thin films identity has been verified. Crystallite size was measured using FWHM of the XRD spectrum. The slimming of the FWHM is inversely proportional to the average crystallite size (D). This could be predicted by the Scherer's formula,

$$D(h) = K\lambda / (\beta \cos\theta),$$

Where, D is the grain size and  $\beta$  is the observed full width at half maximum intensity of the peak. An average value of  $\beta$  has been taken to calculate D. where, it's found that 0.117 nm, 1.834 nm for films annealed for 1hr and 2hrs respectively. The annealed temperature varied with time affected the structural parameters like the lattice constant at 8.2207 for 1hr film and 7.1371 for 2hrs film. The unit cell volume of the films were  $V = 363.55\text{cm}^3$  and  $81.1884\text{ cm}^3$ , However, [15]. Who prepared  $\text{Co}_3\text{O}_4$  thin films by sol-gel and by spin coating technique respectively have found the  $\text{Co}_3\text{O}_4$  thin films were formed in a single-phase, suggesting that  $\text{Co}_3\text{O}_4$  is more stable.

Hamdani et al. (2008) have also obtained a single-phase for  $\text{Co}_3\text{O}_4$  films prepared by spray pyrolysis after annealing temperature, while [2] have observed the appearance of some XRD peak reflections corresponding to  $\text{CoO}$  and  $\text{Co}_2\text{O}_3$  after annealing. The SEM shows the surface morphology of the thin films. The grains were all crystallized and the grain distributions even and thus improve higher conductivity. This may be due to doping and the annealing time of the thin film. This is in line with [1] the grains distributions were evenly distributed. The doping and differences in the annealing time affect the Crystallinity of the films. The increase in thickness shows an improvement in Crystallinity and grain size.

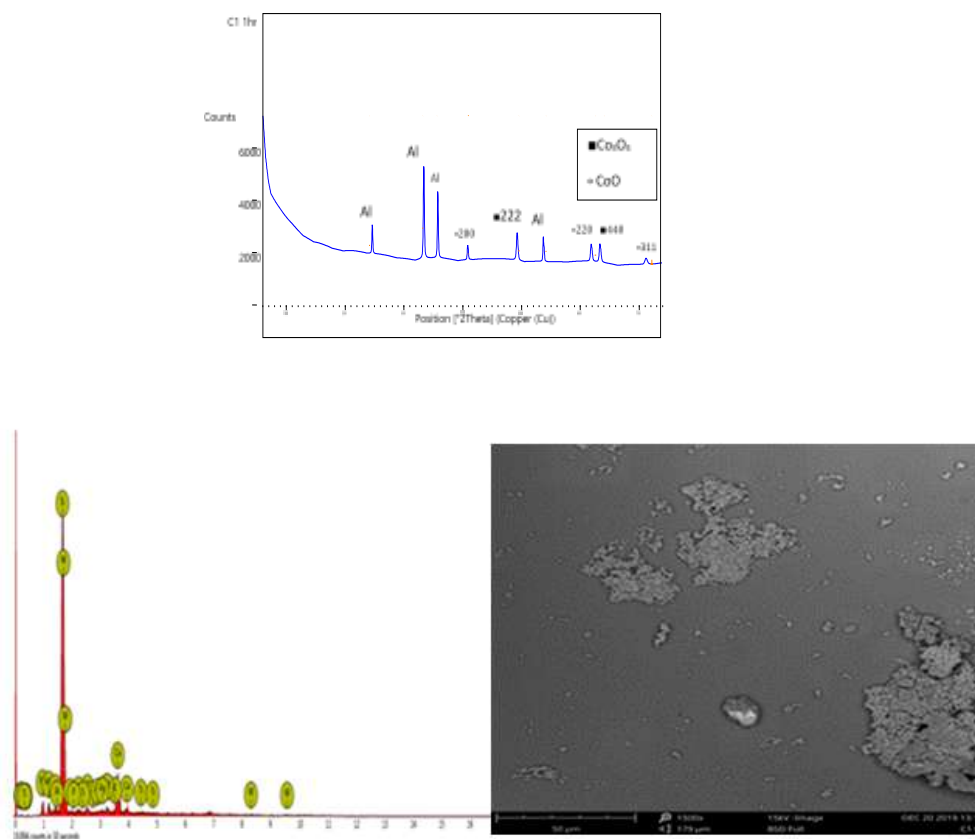


Fig 3.3: SEM Micrograph/EDS for ACO thin films annealed at 1hr

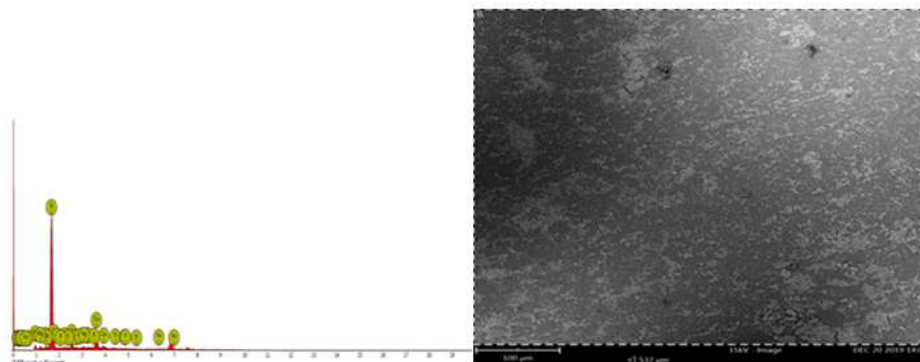


Fig 3.4 SEM micrograph/EDS of ACO thin film annealed at 300°C for 2hrs

Table 3.4a and 3.4b: Composition analysis for ACO thin film annealed for 1hr and 2hrs

(a)

| Element Number | Element Symbol | Element Name | Atomic Conc. | Weight Conc. |
|----------------|----------------|--------------|--------------|--------------|
| 1 4            | S i            | Silicon      | 62.51        | 43.94        |
| 7 4            | C o            | Cobalt       | 4.89         | 22.47        |
| 2 0            | C a            | Calcium      | 14.38        | 14.43        |
| 4 8            | C d            | Cadmium      | 1.64         | 4.60         |
| 4 7            | A g            | Silver       | 1.08         | 2.92         |
| 1 1            | N a            | Sodium       | 3.62         | 2.08         |
| 1 7            | C l            | Chlorine     | 2.16         | 1.91         |
| 1 9            | K              | Potassium    | 1.90         | 1.86         |
| 1 2            | M g            | Magnesium    | 2.54         | 1.54         |
| 1 6            | S              | Sulfur       | 1.70         | 1.36         |
| 1 3            | A l            | Aluminium    | 3.69         | 1.14         |
| 1 5            | P              | Phosphorus   | 1.27         | 0.98         |
| 2 2            | T i            | Titanium     | 0.64         | 0.76         |

(b)

| Element Number | Element Symbol | Element Name | Atomic Conc. | Weight Conc. |
|----------------|----------------|--------------|--------------|--------------|
| 1 4            | S i            | Silicon      | 64.69        | 54.36        |
| 2 0            | C a            | Calcium      | 15.70        | 18.83        |
| 7 4            | C o            | Cobalt       | 2.08         | 6.98         |
| 4 7            | A g            | Silver       | 1.48         | 4.79         |
| 1 7            | C l            | Chlorine     | 4.07         | 4.32         |
| 1 1            | N a            | Sodium       | 3.25         | 2.23         |
| 1 6            | S              | Sulfur       | 1.88         | 1.81         |
| 1 5            | P              | Phosphorus   | 1.53         | 1.41         |
| 1 3            | A l            | Aluminium    | 1.58         | 1.27         |
| 1 2            | M g            | Magnesium    | 1.66         | 1.20         |
| 1 9            | K              | Potassium    | 1.00         | 1.17         |
| 2 2            | T i            | Titanium     | 0.61         | 0.87         |
| 2 3            | V              | Vanadium     | 0.49         | 0.75         |

#### IV. Conclusion

SILAR deposition technique was used to synthesize Al doped CoO (ACO) thin films on glass substrate and annealed at 300 °C with variation in the annealing time. The thin films deposited were characterized to obtain their optical properties such as; spectral absorbance, transmittance, and reflectance. Other solid state properties like extinction coefficient, imaginary dielectric constant, real dielectric constant, and optical conductivity and energy band gaps were also studied. The characterization of these films reveals their potential application in diverse areas. These include; solar energy collection, antireflection coatings, protective coatings, and in electronics. The structural properties of ACO, were characterize using the XRD analysis which revealed that the films are polycrystalline in nature. The crystallite size was found to decrease with increase in annealing time.

SEM micrograph of the ACO thin films reveals that increase in annealing temperature time improved the crystallinity of the films with the grain size evenly distributed. The elemental composition of the film was determined by the Energy Dispersion Spectroscopy (EDS) and clear peaks of cobalt and aluminium were observed. The presence of aluminum could have altered the particle grain size and distribution.

#### References

- [1]. Ananda, K. and Rajendran, V. Morphological and size effect of NiO nanoparticle via solvothermal process and their optical properties. *Material Science and Semi-Conductor Process*, (2011), 14(1) 43-47.
- [2]. Avila A. G., Barrera E. C., Huerta L. A., and Muhl, S. "Structural and Electrical Characterization of Cobalt Oxide Semiconductors. *Solar Energy Material and Solar Cells*, (2004), 82; 269-275. "
- [3]. Bahlawane, N., Premkumar, A. and Kohse, K. "Preparation of doped spinel cobalt oxide thin films and evaluation of their thermal stability. *Chemical Vapor Deposition*", (2007), 13(2-3), 118-122.
- [4]. Bragg, W. H. and Bragg, W. L (1913). "The Reflection of x-rays by crystals" *Proceedings of the Royal Society London. Mathematical, Physical and Engineering Science* (1913), 88; \$28-438.
- [5]. Chougule, M., Palit, V. and Sen, S. "Synthesis and characterization of Co<sub>3</sub>O<sub>4</sub>. Thin films," (2012), 2(1).
- [6]. Ezeokoye, B. A. "Optical properties of CUCL binary thin films deposited by solution growth method". *Greenwich Journal of Science and Technology*, (2003). 4(1): 365-368.
- [7]. Osuwa, J. C. and Oriaku, C. I. Study of physical properties of ternary Cu<sub>11</sub>Cd<sub>4</sub>O thin film glasses. *Chalcogenide Letters*, (2009). 6(8), 385
- [8]. Osuwa, J. C. and Oriaku, C. I. On the Optical Dispersion Parameters of Thin Film Al<sup>3+</sup>doped ZnO. *Transparent of Ovonic Research*, (2010). 5(6): 54-56.
- [9]. Osuwa, J. C. and Uwaezi, U. P. Effects Annealing on the Optical, Structural and Electrical Properties of NiS<sub>2</sub> Thin Film. M.sc Project 2013, Michael Okpara University of Agriculture Umudike.
- [10]. Thi Ly Le. Preparation of transition metal oxide thin films used as solar absorbers. Materials. "Dissertation" Université Paul Sabatier - Toulouse III, English. <NNT : 2016TOU30120>. <tel-01578163>
- [11]. Barrera, L. Huerta, S. Muhl, A. Avila "Synthesis Of Black Cobalt And Tin Oxide Films By The Sol-Gel Process: Surface And Optical Properties" *Solar Energy Material And Solar Sells* Vol 88(2005)179-186
- [12]. M.M Rahman, S. Bahadar Khan., H.M. Marwuni, and A.M. Asiri. "Facile Synthesis of doped ZnO – CdO Nanoblocks as solid – phase adsorbent and efficient solar photo- catalyst application " *J. Ind. Eng. Chem* 2014(20), 2278-2286"
- [13]. T. Xia, M. Kovichich, And A. E. Nel, "Comparison Of Mechanism Of Toxicity Of Zinc Oxide And Cerium Oxide Nanoparticle Based On Dissolution And Oxidation Stress Properties". *ACS Nano* 2008(2) 2592.
- [14]. K.M Shaju, G. Peter, Bruce, "Macroporous Li (Ni<sub>1/3</sub>Co<sub>1/3</sub>Mn<sub>1/3</sub>) O<sub>2</sub>: A High- Rate Positive Electrode For Rechargeable Lithium Batteries" *Journal of Power Source*, 2007(174)1201-1205
- [15]. S, G Kandalkar, C.D Lokhande. R.S. Mane, and S.H Han "A Non- Thermal Chemical Synthesis of Hydrophilic and Amorphous Cobalt Oxide Films for Supercapacitor Application " *Applied Surface Science* 2007(8)3952-3956

K.U, POkpechi, A.D Asiegbu, et. al. "Study of Structural / Optical Properties of Aluminum Doped CoO [ACO] Thin Films." *IOSR Journal of Applied Physics (IOSR-JAP)*, 13(4), 2021, pp. 15-23.